Linkage of Catalysis and Regulation in Enzyme Action. Carbon Isotope Effects, Solvent Isotope Effects, and Proton Inventories for the Unregulated Pyruvate Decarboxylase of *Zymomonas mobilis*

Shaoxian Sun, Ronald G. Duggleby, and Richard L. Schowen*

Contribution from the Department of Chemistry and Higuchi Biosciences Center, University of Kansas, Lawrence, Kansas 66045-0046, and Centre for Protein Structure, Function and Engineering, Department of Biochemistry, University of Queensland, Brisbane 4072, Australia

Received March 2, 1995[⊗]

Abstract: The pyruvate decarboxylase of the bacterium *Zymomonas mobilis* (ZMPDC), in contrast to that of yeast (SCPDC), is not regulated by substrate and shows simple Michaelis–Menten kinetics with rate constants k/B (equivalent to k_{cat}/K_m) and k (equivalent to k_{cat}). C_1-carbon-13 isotope effects obtained by direct measurement with 99% ^{13}C-labeled substrate, which permits determination of the isotope effect on both k/B and k, give $^{13}(k/B) = 1.010 \pm 0.008$ and $^{13}k = 1.019 \pm 0.008$. These are similar to the effects with SCPDC and show that decarboxylation is about 20% rate-limiting at low pyruvate levels and about 40% rate-limiting at high pyruvate levels. From these values, the rate constants for individual events in the catalytic cycle can be estimated (to within about a factor of 2) for ZMPDC: addition of pyruvate to the enzyme, 8×10^5 M^{-1} s^{-1}; off-reaction of pyruvate, 300 s^{-1}; decarboxylation, 1200 s^{-1}; product release, 750 s^{-1}. Solvent isotope effects are small and normal (k/B[HOH]/k/B[DOD] = 1.25 ± 0.05, k[HOH]/k[DOD] = 1.30 ± 0.01), in strong contrast to those for SCPDC (e.g., an inverse isotope effect of 2 on k/B), which were considered to arise from sulfhydryl-addition reactions coupled to regulation. The proton inventories for ZMPDC are also quite different from those for SCPDC. The overall picture suggests that ZMPDC possesses a similar chemical mechanism but somewhat greater catalytic power than SCPDC because of both stronger uniform binding of all states and greater specific stabilization of transition states relative to reactant states. Thus introduction of the regulatory features of SCPDC is coincident with a reduction in catalytic power.

Introduction

Pyruvate decarboxylases (PDCs, EC 4.1.1.1) are enzymes that accelerate by a factor around 10^{12}–10^{13} the reaction of their cofactor thiamin diphosphate (ThDP) with pyruvate to generate

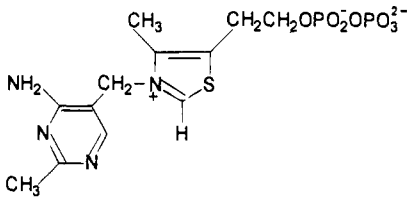

carbon dioxide and acetaldehyde.[1] The enzyme from yeast (*Saccharomyces cerevisiae or carlsbergensis*; SCPDC) is the best studied member of the class; crystal structures of SCPDC and related enzymes have recently appeared and have given rise to mechanistic proposals.[2] We have used substrate isotope effects to estimate the values of the microscopic rate constants for SCPDC action.[3,4] SCPDC is subject to *hysteretic regulation* by a "regulatory molecule" of its substrate pyruvate, the enzyme undergoing a slow activation and then cycling catalytically several thousand times before an inactivation event occurs. Baburina *et al.*[5] have shown that cysteine-221 of SCPDC is required for this behavior, which is abolished by mutation of C221 to serine, in accord with a large body of evidence that sulfhydryl addition to the carbonyl of the regulatory pyruvate is critical for activation of the enzyme.

It had generally been assumed that the slow activation step (characteristic response time of about 10–15 s at 1 mM pyruvate[6]) consisted of a protein conformational change coupled to a sulfhydryl-addition reaction at the carbonyl group of the regulatory pyruvate.[4] In contrast, we have deduced from solvent isotope effects that sulfhydryl addition to the regulatory pyruvate molecule occurs within each catalytic cycle. We hypothesize that this addition reaction is coupled to the opening of the active site to admit pyruvate and that a rapid, subsequent elimination reaction is coupled to closure of the active site, allowing the reactants to be sequestered during the catalytic chemical events.[6] A more complex deduction from solvent isotope effects on the rate constant that is determined in part by product release again

[⊗] Abstract published in *Advance ACS Abstracts*, July 1, 1995.

(1) (a) Kluger, R. *Chem. Rev.* **1987**, *87*, 863–876. (b) Schellenberger, A. *Angew. Chem., Int. Ed. Engl.* **1967**, *6*, 1024–1035. (c) Bisswanger, H., Ullrich, J., Eds. *The Biochemistry and Physiology of Thiamin Diphosphate Enzymes*; VCH Publishers: Weinheim, Germany, 1991. (d) Schellenberger, A., Schowen, R. L., Eds. *Thiamin Pyrophosphate Biochemistry*; CRC Press: Boca Raton, FL, 1988. (e) Thiamin: *Twenty Years of Progress*; Sable, H. Z., Gubler, C. J., Eds.; New York Academy of Sciences: New York, 1982.

(2) (a) Dyda, F.; Furey, W.; Swaminathan, S.; Sax, M.; Farrenkopf, B.; Jordan, F. *Biochemistry* **1993**, *32*, 6165–6170. (b) Muller, Y. A.; Lindqvist, Y.; Furey, W.; Schulz, G. E.; Jordan, F.; Schneider, G. *Structure (London)* **1993**, *1*, 95–103. (c) Lindqvist, Y.; Schneider, G. *Curr. Opin. Struct. Biol.* **1993**, *3*, 896–901. (d) König, S.; Schellenberger, A.; Neef, H.; Schneider, G. *J. Biol. Chem.* **1994**, *269*, 10879–10882 and references given in these papers.

(3) Alvarez, F. J.; Ermer, J.; Hübner, G.; Schellenberger, A.; Schowen, R. L. *J. Am. Chem. Soc.* **1991**, *113*, 8402–8409.

(4) Huhta, D. W.; Heckenthaler, T.; Alvarez, F. J.; Ermer, J.; Hübner, G.; Schellenberger, A.; Schowen, R. L. *Acta Chem. Scand.* **1992**, *46*, 778–788.

(5) Baburina, I.; Gao, Y.; Jordan, F.; Hohmann, S.; Furey, W. *Biochemistry* **1994**, *33*, 5630–5635.

(6) Alvarez, F. J.; Ermer, J.; Hübner, G.; Schellenberger, A.; Schowen, R. L. *J. Am. Chem. Soc.* **1995**, *117*, 1678–1683.

0002-7863/95/1517-7317$09.00/0

suggested an addition reaction of sulfhydryl to carbonyl, which we hypothesize to be coupled to opening of the active site to allow departure of the product acetaldehyde.[6]

The bacterium *Zymomonas mobilis* possesses a pyruvate decarboxylase (ZMPDC) that is structurally and chemically similar to SCPDC except for the absence of regulation: the signs of hysteretic regulation (slow activation of the enzyme after addition of substrate to the reaction mixture; sigmoid saturation plot of initial rate against pyruvate concentration) are missing in ZMPDC.[7a] Instead, ZMPDC exhibits immediately linear initial rates of product formation and hyperbolic dependence of initial rate on pyruvate concentration. In agreement with evidence that regulation in SCPDC is governed by interaction with C221, there are no cysteine residues in the corresponding region of ZMPDC.[7]

ZMPDC should therefore lack also the solvent isotope-effect signature of regulation through sulfhydryl addition to a regulatory-pyruvate carbonyl: inverse isotope-effect contributions arising from the loosely-bound reactant-state sulfhydryl site.[6] We report here the measurement of solvent isotope effects and proton inventories with ZMPDC.

C_1-carbon isotope effects on the observable rate constants are a measure of the kinetic significance of decarboxylation in the processes described by these rate constants. In previous work with SCPDC, ^{13}C-isotope effects were determined by two different techniques. Competitive measurements[8] with use of the isotope-ratio mass spectrometer gave very precise results which inevitably reflect both the isotope competition in formation of enzyme-bound species and isotopic competition in further reactions of the enzyme complexes up to and including the first irreversible step (which ends the competition) but not beyond. The isotope effect was somewhat less than 1%. On the assumption that the model-reaction isotope effect[9] of 5% is roughly valid for enzymic decarboxylation, this result indicates that the kinetic significance of the decarboxylation transition state in events between activated enzyme and decarboxylation is a little less than 20% (the decarboxylation process is less than 20% rate-limiting for the first part of the reaction).[3]

Direct rate measurements for ^{12}C-substrate and fully-labeled ^{13}C-substrate were also carried out.[3] This method yields less precise isotope effects, but in contrast to the competitive method, it allows the determination of effects on all the individual rate parameters.[10] For the early phase of the reaction, which is rate-limiting at low pyruvate concentrations and involves binding of substrate into the active site and all subsequent events through the decarboxylation transition state, the isotope effects are the same for both competitive and direct methods; they indicate, as described above, decarboxylation to be about 20% rate-limiting. The rate for the late phase of the reaction, under conditions of enzyme saturation, is potentially determined by decarboxylation and/or product release. The directly measured isotope effect for this phase of the reaction (information not accessible in competitive studies) is 2.5%. Again, on the assumption of an intrinsic isotope effect of 5% for the decarboxylation step, this indicates a kinetic significance of 50% for decarboxylation (and thus a kinetic significance of 50% for product release): in this late phase of the catalytic cycle, decarboxylation and product release therefore proceed at about equal rates.[3] Such considerations allowed the estimation of rate constants for the individual reaction steps in SCPDC action. In the present paper we also report directly measured ^{13}C-isotope effects for ZMPDC.

Experimental Section

Materials. Thiamin diphosphate hydrochloride ("cocarboxylase"), sodium pyruvate (anhydrous), and NADH were purchased from Sigma, sodium pyruvate-*1*-^{13}C (anhydrous, 99% ^{13}C) from Cambridge Isotope Co., anhydrous citric acid from Fisher, and sodium citrate dihydrate and magnesium sulfate (anhydrous) from J. T. Baker. Deuterium oxide was from Aldrich (99.9% D). Both sodium pyruvate and sodium pyruvate-*1*-^{13}C were 10% hydrated in aqueous solution (NMR).[11]

Enzymes. Pyruvate decarboxylase (EC 4.1.1.1) from *S. carlsbergensis* (specific activity, 9 units/mg; specific activity of the pure enzyme,[12] 80 units/mg) was purchased from Sigma and suspended in a solution of 5% glycerol, 3.2 M ammonium sulfate, 5 mM potassium phosphate, 1 mM magnesium acetate, 0.5 mM EDTA, and 25 μM ThDP (pH 6.5). Alcohol dehydrogenase (EC 1.1.1.1) from baker's yeast was also obtained from Sigma with a specific activity of 360 units/mg. Pyruvate decarboxylase[13] from *Z. mobilis* was isolated with a specific activity of 62 units/mg and stored in 50% glycerol solution at −20 °C. The enzyme activity showed no change over several months. The specific activity of the pure enzyme is 115 units/mg.[13]

Kinetic Method. The decarboxylation of pyruvate with pyruvate decarboxylase, coupled to acetaldehyde reduction by NADH catalyzed by alcohol dehydrogenase, was followed (360 nm; $\epsilon = 3670\ M^{-1}\ cm^{-1}$; at this wavelength, initial absorbance was always <1.2 and the contribution of pyruvate to the absorbance was smaller than at 340 nm) with use of a Shimadzu 160U UV/vis spectrophotometer interfaced to an IBM-compatible computer. The reaction was initiated by addition of a sodium pyruvate solution to a solution of all other materials in a 1-mL cuvet. The final concentrations for the SCPDC reaction were as follows: SCPDC,[12] 0.035 units/mL; ThDP, 5 mM; $MgSO_4$, 5 mM; NADH, 0.256 mM; ADH, 30 units/mL; sodium pyruvate 0.2−30 mM; citrate buffer, 0.1 M (pH 6.0). Concentrations for the ZMPDC reaction: ZMPDC,[13] 0.058 units/mL; ThDP, 0.1 mM; $MgSO_4$, 5 mM; NADH, 0.256 mM; ADH, 10 units/mL; sodium pyruvate, 0.1−30 mM; citrate buffer, 0.1 M (pH 6.2). All reactions were conducted at 30.0 ± 0.1 °C. Absorbance data were collected by the Shimadzu data-acquisition program at time intervals of 1 s for 200 s.

Kinetic Technique for Solvent Isotope Effects. Buffers were prepared[17] with the use of either pure H_2O or 99.9% D_2O as solvent. Overall solvent isotope effects were calculated from the kinetic parameters measured in 99.9% D_2O buffers and H_2O buffers. In proton inventory studies, mixture of appropriate volumes of D_2O buffer and H_2O buffer gave the required atom fraction of deuterium.

Kinetic Technique for ^{13}C-Isotope Effects. Rates were measured with otherwise identical solutions using the same concentrations of ^{13}C-labeled pyruvate and of unlabeled pyruvate. Experiments employing these identical solutions were run simultaneously and in parallel in order to achieve an optimal cancellation of errors between measurements with the two isotopic substrates. The ratio of the velocities then gave the ^{13}C-isotope effect ^{13}v for the chosen pyruvate concentration *S*. Equation[14] 1 was used to obtain $^{13}(k/B)$ and ^{13}k from ^{13}v as a function of *S*.

(7) (a) Miczka, G.; Vernau, J.; Kula, M.-R.; Hofmann, B.; Schomburg, D. *Biotech. Appl. Biochem.* **1992**, *15*, 192−206. Miczka et al. observe sigmoid kinetics (Hill coefficient of 1.8) for ZMPDC but cite the work of Neale et al. (Neale, A. D.; Scopes, R. K.; Wettenhall, R. E. H.; Hoogenraad, N. J. *J. Bacteriol.* **1987**, *169*, 1024−1028) and of Hoppner and Doelle (Hoppner, T. C.; Doelle, H. W. *Eur. J. Appl. Microbiol. Biotechnol.* **1983**, *17*, 152−157), in which hyperbolic kinetics was found. We confirm the hyperbolic kinetics for ZMPDC (see below). (b) Green, J. B. A. *FEBS Lett.* **1989**, *246*, 1−5.

(8) (a) O'Leary, M. H. *Biochem. Biophys. Res. Commun.* **1976**, *73*, 614−618. (b) Jordan, F.; Kuo, D. J.; Monse, E. U. *J. Am. Chem. Soc.* **1978**, *100*, 2872−2878. (c) DeNiro, M. J.; Epstein, S. *Science* **1977**, *197*, 261−263.

(9) Jordan, F.; Kuo, D. J.; Monse, E. U. *J. Am. Chem. Soc.* **1978**, *100*, 2872−2878.

(10) Schowen, R. L.; Schowen, K. B. In *Stable Isotopes in the Biosphere*; Wada, E., Yoneyama, T., Minagawa, M., Ando, T., Eds.; Kyoto University Press: Kyoto, Japan, 1993.

(11) Kokesh, F. C. *J. Org. Chem.* **1976**, *41*, 3593−3599.

(12) Ullrich, J. *Methods Enzymol.* **1970**, *18A*, 109−115. Zehender, H.; Trescher, D.; Ullrich, J. *Eur. J. Biochem.* **1987**, *167*, 149−154. One unit of SCPDC produces 1 μmol min^{-1} of product at pH 6.0, 30 °C, saturating substrate.

(13) Diefenbach, R. J.; Duggleby, R. G. *Biochem. J.* **1991**, *276*, 439−445. One unit of ZMPDC activity produces 1 μmol min^{-1} of product at pH 6.5, 30 °C, saturating substrate. SCPDC exhibits identical rates at pH 6.0 and 6.5, so one ZMPDC unit equals one SCPDC unit.[12]

(14) Stein, R. L. *J. Org. Chem.* **1981**, *46*, 3328−3330.

$$^{13}v = \{B/(B + S)\}^{13}(k/B) + \{S/(B + S)\}^{13}k \quad (1)$$

The use of eq 1 in place of independently fitting v_{12} and v_{13} to the Michaelis–Menten equation preserves the precision obtained by parallel experiments using identical solutions. Here, k is analogous to k_{cat} and B to K_m; the two correspond to the terms similarly denoted in the more complex rate law for SCPDC.[3,6]

Data Reduction. Initial rates for ZMPDC were calculated from absorbance vs time data fit to a straight line using the DERIV program (a linear least-squares program). For SCPDC, the initial activation phase was allowed to pass and the data were then fit to a straight line to obtain the initial rate. Kinetic parameters were determined by fitting velocity vs substrate concentrations to eq 2 for SCPDC and eq 3 for ZMPDC using the SIGMA-PLOT program (nonlinear least-squares fitting), and a weighting factor of $1/v$ was applied.

$$v/[\text{SCPDC}]_o = kS^2/[A + BS + S^2(1 + S/K_i)] \quad (2)$$

$$v/[\text{ZMPDC}]_o = kS/[B + S(1 + S/K_i)] \quad (3)$$

Results

Comparative Kinetics of SCPDC and ZMPDC. Typical data for the initial specific velocity $v/[\text{enzyme}]_o$ as a function of S are shown in Figure 1, confirming the sigmoid behavior of SCPDC and the hyperbolic behavior of ZMPDC. The resulting values of k (analogous to k_{cat}) were adjusted to a value of 320 s^{-1} for SCPDC[3] and 460 s^{-1} for ZMPDC (calculated for the tetramer as active species by taking the activity of pure ZMPDC[13] as 115 units/mg and the molecular mass as 240 kDa). As before,[3,6] SCPDC action is described by four kinetic parameters (k, A, B, and the substrate-inhibition constant K_i in eq 2), while the simpler kinetics of ZMPDC requires only three (k, B, and K_i in eq 3; although the customary symbols k_{cat} and K_m might have been employed with ZMPDC, we use k and B to emphasize the similarities with the corresponding terms in the more complex rate law for SCPDC). For SCPDC, K_i was fixed at 264 mM as previously determined,[3] yielding values of the other kinetic parameters in general agreement with earlier measurements[3] (k/A, $1.55 \pm 0.06 \times 10^8$ vs $1.17 \pm 0.03 \times 10^8$ M^{-2} s^{-1}; k/B, $2.19 \pm 0.09 \times 10^5$ vs $2.34 \pm 0.12 \times 10^5$ M^{-1} s^{-1}; k was adjusted to a value of 320 s^{-1} in both cases). For ZMPDC, K_i was first obtained from fits to eq 3 and the mean value of 579 mM was used in calculating $k = 460 \pm 4$ s^{-1}, $B = 0.74 \pm 0.02$ mM, and $k/B = 6.19 \pm 0.19 \times 10^5$ M^{-1} s^{-1}.

Carbon Isotope Effects. As described above, paired experiments were conducted with ^{13}C- and ^{12}C-substrates, so that ratios $v_{12}/v_{13} = {}^{13}v$ at various substrate concentrations S were as nearly independent of variations in enzyme activity, reaction conditions, etc., as possible. The results are shown in Table 1. The isotope effects $^{13}(k/B)$ and ^{13}k were then obtained by fitting ^{13}v (S) to eq 1 above.

Figure 2 shows a plot of ^{13}v vs $\{S/(S + B)\}$, the intercepts of which yield $^{13}(k/B) = 1.010$ and $^{13}k = 1.019$. The fitting of the mean values of ^{13}v to eq 1 yields standard errors in these isotope effects of 0.003 and 0.002, respectively, but these are underestimates because they neglect the errors in ^{13}v. We therefore ascribe error limits equal to the average standard error in the values of ^{13}v: thus, $^{13}(k/B) = 1.010 \pm 0.008$ and $^{13}k = 1.019 \pm 0.008$.

Solvent Isotope Effects and Proton Inventories for ZMPDC. The steady-state kinetics for ZMPDC were characterized in mixtures of HOH and DOD. The results are shown in Table 2 and Figures 3 (k/B) and 4 (k). The overall isotope effects on both parameters are normal and small: $^{DOD}(k/B) = 1.25 \pm 0.05$ and $^{DOD}k = 1.30 \pm 0.01$.

Discussion

Carbon Isotope Effects: Calculation of Microscopic Rate Constants. Chart 1 shows a very simple scheme for binding of pyruvate to ZMPDC (on-rate constant (k_{c1}), off-rate constant (k_{c2}), decarboxylation (k_{c3}), and product release (k_{c5})). The notation here is kept analogous to that employed for the catalytic cycle of SCPDC (for the reactions of which all rate constants were marked by a subscript c) after its activation by a regulatory molecule of pyruvate (all rate constants for activation reactions were marked by a subscript a).[3,4,6] It should be noted that, although the catalytic cycle is divided into the three minimal components (substrate binding, chemical step, and product

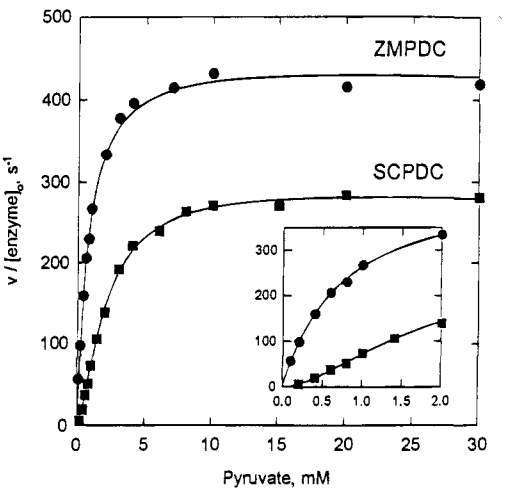

Figure 1. ZMPDC exhibits hyperbolic kinetics with weak substrate inhibition while SCPDC exhibits sigmoidal kinetics with weak substrate inhibition. The inset shows the clear contrast between hyperbolic and sigmoidal kinetics at the lowest pyruvate concentrations. The data are given in Table S1 of the supporting information. The solid lines are plots of eqs 2 (SCPDC) and 3 (ZMPDC).

Table 1. Velocity Ratios v_{12}/v_{13} for Decarboxylation of $^{13}C_1$-Labeled Pyruvate with Catalysis by ZMPDC as a Function of Pyruvate Concentration[a]

[pyruvate], mM	$v_{12}/v_{13} \pm$ SE (N_{12}, N_{13})[b]	[pyruvate], mM	$v_{12}/v_{13} \pm$ SE (N_{12}, N_{13})[b]
0.40	1.013 ± 0.010 (5, 5)	10.0	1.020 ± 0.010 (8, 8)
0.80	1.016 ± 0.006 (5, 5)	15.0	1.019 ± 0.007 (6, 6)
4.00	1.014 ± 0.008 (7, 7)		

[a] ZMPDC, 0.058 units/mL; yeast alcohol dehydrogenase, 10 units/mL; $MgSO_4$, 5 mM, ThDP, 0.1 mM; pH 6.2, 0.1 M citrate buffer; temperature, 30.0 °C. [b] SE = standard error, N = number of runs.

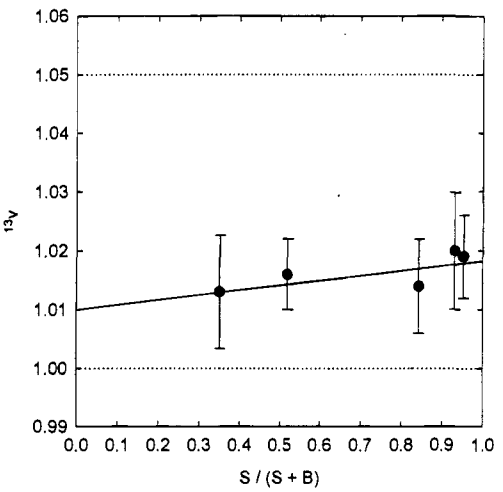

Figure 2. Extrapolation of observed carbon isotope effects ^{13}v to $S/(S + B) = 0$, which gives $^{13}(k/B)$, and to $S/(S + B) = 1$, which gives ^{13}k. The data are from Table 1. The solid line gives the least-squares fit to eq 1. The dotted line give the probable limits of the intrinsic isotope effects for steps in which no C_1–C_2 bond fission occurs ($^{13}v = 1.00$, lower limit) and for the decarboxylation step ($^{13}v = 1.05$, upper limit).

Table 2. Steady-State Kinetic Parameters for the Decarboxylation of Pyruvate with Catalysis by ZMPDC as a Function of Atom Fraction of Deuterium in Mixtures of Protium and Deuterium Oxides[a]

atom fraction of deuterium, n[b]	B (SE), mM	k (SE), s^{-1}	10^{-3} k/B (SE), M^{-1} s^{-1}
0.00	0.743 (0.022)	460 (4)	619 (19)
0.15	0.712 (0.020)	439 (4)	617 (18)
0.30	0.723 (0.026)	421 (4)	582 (22)
0.40	0.717 (0.021)	419 (3)	585 (18)
0.50	0.701 (0.020)	412 (3)	588 (17)
0.59	0.693 (0.014)	395 (2)	570 (12)
0.69	0.692 (0.014)	379 (2)	547 (11)
0.84	0.716 (0.029)	361 (4)	504 (21)
0.99	0.715 (0.024)	352 (3)	493 (17)

[a] Experimental conditions are identical to those for Table 1. [b] The values of n have been corrected for protium introduced in buffer preparation and by enzyme stock solutions.

release) and each component is assigned a microscopic rate constant (*i.e.*, a constant not directly accessible from the reaction kinetics), each of the microscopic rate constants is very likely to describe a complex array of serial and parallel events that make up the overall process designated by the rate constant.

Chart 1 also gives the definitions of the observable steady-state rate constants k/B and k in terms of the four microscopic rate constants. The two observable ^{13}C-isotope effects are shown in their relationship to the microscopic rate constants and the intrinsic isotope effects on the individual steps ($^{13}k_{c1}$, ..., $^{13}k_{c5}$). Here we use the weighting-factor formulation of Stein[14] (mathematically equivalent to the Northrop formulation[15]), in which the observed isotope effect on a series of steps is just the weighted average of the intrinsic isotope effects. The weighting factor for any step is then the fraction by which that step limits the rate.

The calculations shown in Chart 1 begin with an estimate[16] that the intrinsic ^{13}C-isotope effect for decarboxylation has a probable value of 1.05 and lies between the limits of 1.03 and 1.07 and that the intrinsic ^{13}C-isotope effect on all other steps is 1.00. The microscopic constants are calculated using the upper and lower limits as well as the probable value. The experimental errors in the observed effects are relatively unimportant because of the large range of values for the microscopic rate constants that is dictated by the uncertainty in the intrinsic isotope effect for decarboxylation. Chart 1 shows that, generally, the microscopic rate constants are estimated to within a factor of about 2.

Proton Inventory for k/B, ZMPDC. The proton inventory for k/B is shown in Figure 3 (left), with the comparable proton inventory for SCPDC, determined in previous work,[6] shown in Figure 3 (right) for comparison. There is a stark contrast between the two results.

SCPDC shows an inverse isotope effect, faster in deuterium oxide by a factor of 2.3. The proton inventory for SCPDC can be fitted to the equation shown in Figure 3 (right) (solid curve), in which the decarboxylation event (weighting factor of 0.15, derived from the ^{13}C-isotope effect) is assumed to contribute no solvent isotope effect, and the substrate-binding event (weighting factor of 0.85) to contribute the entire isotope effect. We consider the isotope effect on substrate binding to arise from sulfhydryl addition to the pyruvate molecule at the regulatory site, with this addition being a prerequisite for entry of the substrate pyruvate molecule into the active site. The line through the data is generated from a model according to which a loosely-bound reactant-state site (a sulfhydryl group with fractionation factor of $^1/_3$ in our model[18]) is transformed into a tightly-bound transition-state site (the hydroxyl group of the (*S*)-α-lactylcysteine derived from the activating substrate molecule bound at the regulatory site).[6] This addition necessarily occurs within every catalytic cycle, and we took it to be linked to the opening of the active site to admit each new substrate molecule, with the addition reaction perhaps providing the energy to drive the opening event.

ZMPDC shows a small normal isotope effect, faster in protium oxide by a factor of 1.25. Here the proton inventory is slightly "dome-shaped," in contrast to the bowl-shaped "hypercurvature" found for SCPDC. Such small isotope effects are difficult to interpret. One simple model that fits the data is this: a step with a multiproton isotope effect of 3.5 ("medium effect", generalized solvation or protein-conformational effect) is rate-limiting to the extent of 10%, while other steps (90% rate-limiting) generate no solvent isotope effect.[19] The function corresponding to this model is plotted in Figure 3 (left), but the model should be taken as purely illustrative. Many other models will fit equally well.

Proton Inventory for k, ZMPDC. The proton inventory is shown in Figure 4 (left); the comparable proton inventory[6] for SCPDC is shown in Figure 4 (right). Here again there is a strong contrast between the results for the two enzymes. This rate constant reflects both decarboxylation and product release in about equal proportions (i.e., both occur at about equal rates) for both enzymes, as indicated by the ^{13}C-isotope effects of 1.025 and 1.019.

The proton inventory for SCPDC is "hypercurved" (the data show curvature greater than the exponential curvature that is limiting for kinetically simple cases).[6,17] These data have been interpreted[6] to indicate that addition of a sulfhydryl group to the carbonyl of the regulatory pyruvate is coupled to product release (one-proton inverse isotope effect of 2, offset by a normal many-proton transition-state isotope effect of 4.1), producing the dotted curve of Figure 4 (right), which fits a substantial part of the data.[6] Fits of similar quality can be obtained by taking the sulfhydryl fractionation factor to be $^1/_3$ instead of $^1/_2$ as was done above (line of dots and dashes) in Figure 4 (right); the actual fractionation factor for sulfhydryl is uncertain by at least this amount.

Although the overall isotope effect on k is normal in both cases and similar in magnitude for ZMPDC (1.3) and SCPDC (1.5), the proton inventories indicate a quite different mechanistic origin of the effects. In Figure 4 (left), the dotted line corresponds to the model adopted for SCPDC: decarboxylation (40% rate-limiting) generating no solvent isotope effect, product release (60% rate-limiting) with an overall effect of 1.5 that arises from the cancellation of an inverse one-proton isotope effect of 3 (sulfhydryl addition) by a normal isotope effect of 4.5 ("medium" or protein conformational effect). The line is inconsistent with all of the data for ZMPDC.

Much simpler models give a better account of the results. The dashed line of Figure 4 (left) ascribes a normal isotope effect of 1.5 on product release to a single proton, while the

(15) Northrop, D. B. *Biochemistry* **1975**, *14*, 2644–2650.

(16) In footnote 13 of ref 3, a survey of ^{13}C-isotope effects was given for reactions where decarboxylation is probably fully rate-limiting. The values all fall in the range 1.03–1.07.

(17) Schowen, K. B.; Schowen, R. L. *Methods Enzymol.* **1982**, *87c*, 551–606. Quinn, D. M.; Sutton, L. D. In *Enzyme Mechanism from Isotope Effects*; Cook, P. F., Ed.; CRC Press: Boca Raton, FL, 1991.

(18) In ref 6, the proton inventory of k/B for SCPDC was treated by assuming the weighting factor for substrate binding to be about unity rather than 0.85, making the fractionation factor of the sulfhydryl group 1/2.3 rather than 1/3. There was no difference in the quality of the fit nor in the interpretation of the results.

(19) Although this arbitrarily-chosen function fits the data adequately, other mechanistically significant functions can also be fitted to the data. Among these are models involving ThDP with a nonequilibrium H/D ratio arising from isotope effects on its hydronation during each catalytic cycle. These models are under study and will be described elsewhere.

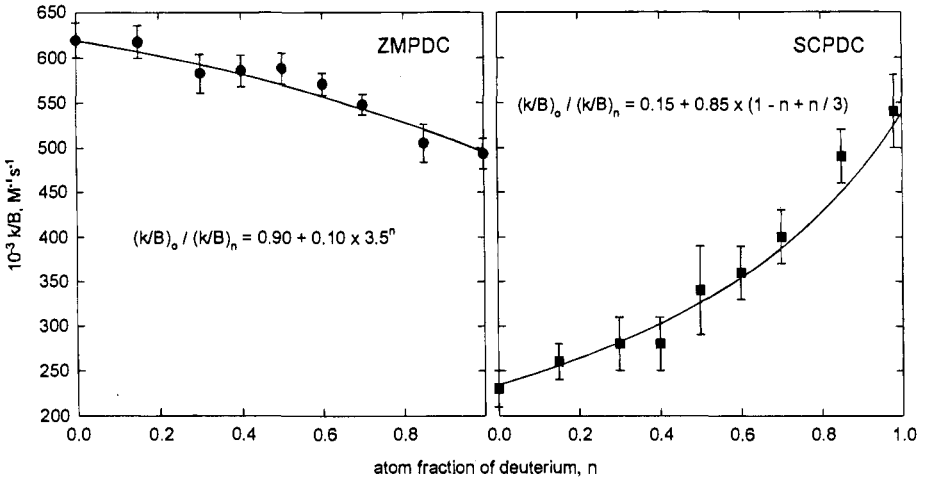

Figure 3. (left panel) Proton inventory on *k/B* for ZMPDC exhibiting a slightly "dome-shaped" curve with a normal isotope effect. The solid line is a plot of the equation shown in the graph. (right panel) Proton inventory on *k/B* for SCPDC exhibiting a bowl-shaped curve with an inverse isotope effect. The solid line is a plot of the equation shown in the graph.

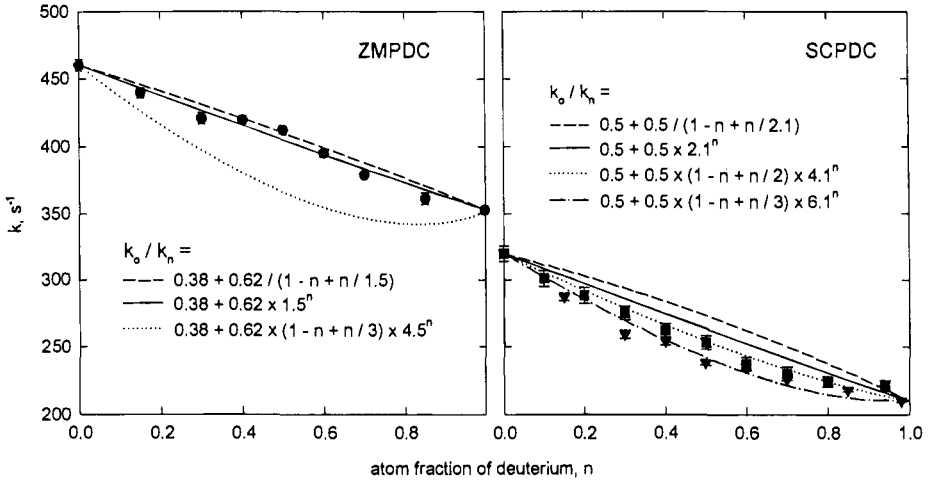

Figure 4. (left panel) Proton inventory on *k* for ZMPDC exhibiting a normal isotope effect of about 1.3. (right panel) Proton inventory on *k* for SCPDC exhibiting "hypercurvature" with a normal isotope effect of 1.5. The lowest curves (dots and dashes; dots) for SCPDC were calculated[6] from a model with (a) decarboxylation and product release equally rate-limiting (weighting factors of 0.5); (b) solvent isotope effect of 1.0 for decarboxylation; (c) one-proton reactant-state fractionation factor of $^1/_3$ (dots and dashes) or $^1/_2$ (dots) in product release; (d) multiproton transition-state isotope effect of 6.1 (dots and dashes) or 4.1 (dots). The other two lines for SCPDC show that simpler models do not account for the data: multiproton isotope effect of 2.1 on product release (solid line) or one-proton isotope effect of 2.1 on product release (dashes). For ZMPDC, the dotted line shows that the SCPDC model, when adapted to ZMPDC, disagrees radically with the data. Here, however, simple one-proton or (better) multiproton models for product release give good agreement.

solid line ascribes the effect to many protons, as in a protein-conformation change. Both lines pass closer to the data than that for the SCPDC-like model with the conformation-change model passing directly among the points. Most simply, therefore, the normal isotope effect of 1.3 on the rate constant *k* for ZMPDC can be considered a weighted average of an effect of 1.0 for decarboxylation and an effect of 1.5 for product release, with the latter of uncertain origin but possibly a combination of many small effects from protein conformational reorganization.

Mechanistic Comparisons and Contrasts between ZMPDC and SCPDC. The basic catalytic mechanism and relative values of rate constants for the mechanistic steps are the same for SCPDC and ZMPDC. SCPDC superimposes upon this common catalytic mechanism the regulatory opening and closing of the active site. The chief kinetic consequence of this regulation is a loss of catalytic power by SCPDC relative to ZMPDC.

The opening and closing of the active site, induced in SCPDC by sulfhydryl addition to the regulatory pyruvate molecule, must not be coupled to exclusion of water from the active site and the resulting hydrophobic acceleration of the decarboxylation reaction.[20] We previously suggested[6] that the regulatory closure of the active site might sequester the reacting ThDP−pyruvate adduct from solvent, but this is clearly incorrect. If regulatory closure produced the hydrophobic character of the active site, then ZMPDC, which lacks the regulatory apparatus, would exhibit different catalytic features and would probably react more slowly than SCPDC. In fact, ZMPDC reacts with very similar catalytic chemistry and more rapidly than SCPDC. This most simply indicates that the regulatory opening/closing in SCPDC must constitute a mechanism for deactivation of the enzyme, i.e., for reducing the catalytic activity at low pyruvate concentrations, as argued below. Such a hypothesis is also consistent with the relatively high catalytic activity (about 15% of the wild-type activity) retained by the unregulated C221S mutant of SCPDC.[5]

Reversible sequestration of the ThDP−pyruvate adduct from the aqueous solvent prior to the decarboxylation reaction seems likely to occur within the catalytic cycles of both ZMPDC and SCPDC; for the latter, it would be independent of the regulatory closure. It was earlier suggested by Kluger and Smyth[21] that the exergonic addition of ThDP to pyruvate might be used to

(20) Crosby, J.; Stone, R.; Lienhard, G. E. *J. Am. Chem. Soc.* **1970**, *92*, 2891−2900. Crosby, J.; Lienhard, G. E. *Ibid.* **1970**, *92*, 5705−5716.

Chart 1

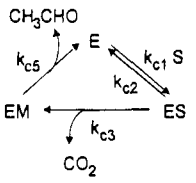

$(k/B) = k_{c1}k_{c3}/(k_{c2}+k_{c3})$ $\quad k = k_{c3}k_{c5}/(k_{c3}+k_{c5})$

$^{13}(k/B) = [k_{c3}/(k_{c2}+k_{c3})]\,{}^{13}k_{c1} + [k_{c2}/(k_{c2}+k_{c3})]\,{}^{13}(k_{c1}k_{c3}/k_{c2})$

$^{13}k = [k_{c5}/(k_{c3}+k_{c5})]\,{}^{13}k_{c3} + [k_{c3}/(k_{c3}+k_{c5})]\,{}^{13}k_{c5}$

Taking:

$^{13}k_{c1} = {}^{13}k_{c5} = 1.00$

$^{13}(k_{c1}k_{c3}/k_{c2}) = {}^{13}k_{c3} = 1.05$ (probable value); 1.03, 1.07 (probable limits)

For the probable $^{13}k_{c3} = 1.05$

$k_{c2}/(k_{c2}+k_{c3}) = [^{13}(k/B) - 1]/0.05$

$k_{c5}/(k_{c3}+k_{c5}) = [^{13}k - 1]/0.05$

Since $^{13}(k/B) = 1.010 \pm 0.008$; $^{13}k = 1.019 \pm 0.008$

$k_{c1} = 8 \times 10^5\ M^{-1}s^{-1}$ $\quad k_{c3} = 1200\ s^{-1}$

$k_{c2} = 300\ s^{-1}$ $\quad k_{c5} = 750\ s^{-1}$ } Probable values

For the limits $^{13}k_{c3} = 1.03, 1.07$

$k_{c1} = 9, 7 \times 10^5\ M^{-1}s^{-1}$ $\quad k_{c3} = 700, 1700\ s^{-1}$

$k_{c2} = 600, 300\ s^{-1}$ $\quad k_{c5} = 1200, 600\ s^{-1}$ } Limiting values

drive the sequestration, leading to the kind of enveloped transition state described by Wolfenden.[22] This very attractive mechanism may indeed prevail for both enzymes.

These points are illustrated in Figure 5 by means of free-energy/reaction progress diagrams[4] for the non-enzymic reaction (constructed from the studies of Washabaugh and Jencks[23] and Kluger et al.[24]), for the hysteretically regulated SCPDC, and for the unregulated ZMPDC. Perhaps the most notable point is that ZMPDC clearly exhibits the highest flux and the greatest amount of stabilization for all transition states along the reaction path. This shows that the introduction of the regulatory apparatus in SCPDC has been accompanied by a decrease in catalytic power. A good part of the advantage of ZMPDC is in uniform binding[25] of transition states and reactant states, a consequence of its greater affinity[13] for ThDP (−20 vs −10 kJ/mol for SCPDC).

The regulatory-activation barrier that precedes the catalytic cycle for SCPDC, requiring that regulatory pyruvate binding precede the onset of catalysis, introduces the sigmoidal activation characteristic apparent in Figure 1 for SCPDC but not for ZMPDC. This feature makes the catalytic advantage of ZMPDC over SCPDC strongly dependent on the pyruvate concentration. At 10 mM pyruvate, ZMPDC is about 1.7 times as active as SCPDC, while at 0.5 mM pyruvate, the ratio is around 10. In addition to this steady-state effect, the hysteretic character of the activation/deactivation follows from the fact that the transition state for the regulatory barrier is higher in free energy by around 20 kJ/mol than any transition state within the catalytic cycle. The catalytic cycle thus occurs several thousand times

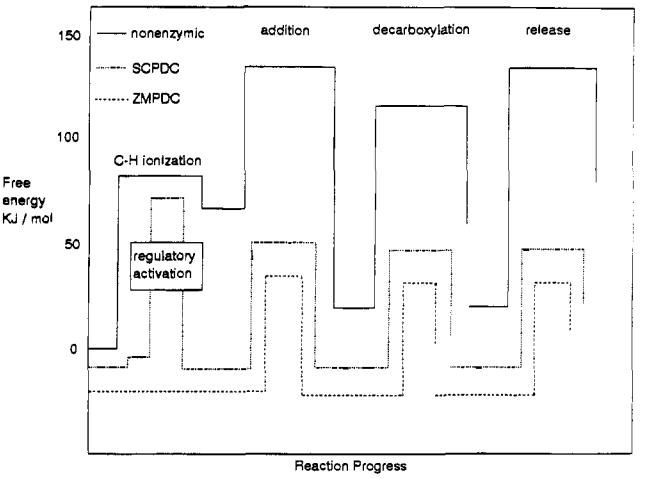

Figure 5. Free-energy diagrams for the non-enzymic decarboxylation of pyruvate[4] (solid line), for SCPDC-catalyzed decarboxylation of pyruvate[4] (dotted line), and for ZMPDC-catalyzed decarboxylation of pyruvate (dashed line). The relative reactant-state free energy for product release is arbitrarily set equal to the relative reactant-state energy for decarboxylation in all three cases. All curves are for standard-state concentrations of 1 mM for pyruvate and ThDP, pH 6.2, and 298 K. The data and calculations are given in Table S3 of the supporting information.

for each regulatory event. The response of the catalytic steady state to rapid fluctuations in the ambient pyruvate concentration is thereby strongly buffered, the characteristic response time being around 10−15 s at 1 mM pyruvate.

The overall effect of the SCPDC regulation thus appears to be an insulation of the catalytic steady state from fluctuations in pyruvate concentration that occur within a period of up to 30 s or so, while providing for a rather sharp shutdown of activity for sustained deficits in pyruvate levels below a few millimolar. ZMPDC, in contrast, maintains a consistent, high activity down to 2−3 mM pyruvate, and below that level, the activity drops linearly, with a response time in all cases not much above the millisecond range.

These differences in regulation may well reflect differences in the role played by pyruvate decarboxylase in the energy economies of *Saccharomyces* and of *Zymomonas*. Whether the contrasts noted between SCPDC and ZMPDC will be general for regulated and unregulated PDCs must await examination of enzymes from other species. We expect to address these matters elsewhere.

Acknowledgment. The work in Lawrence was supported by the U.S. National Institute of General Medical Sciences under Grant No. GM 20198. The work in Brisbane was funded by the Australian Research Council.

Supporting Information Available: Tables of specific velocities for the decarboxylation of pyruvate with catalysis by ZMPDC and by SCPDC as a function of pyruvate concentration and of initial velocities with pyruvate-*1*-^{12}C and pyruvate-*1*-^{13}C as a function of pyruvate concentration and data for the free energy diagrams (4 pages). This material is contained in many libraries on microfiche, immediately follows this article in the microfilm version of the journal, can be ordered from the ACS, and can be downloaded from the Internet; see any current masthead page for ordering information and Internet access instructions.

JA950695H

(21) Kluger, R.; Smyth, T. *J. Am. Chem. Soc.* **1981**, *103*, 1214−1216.
(22) Wolfenden, R. *Mol. Cell. Biochem.* **1974**, *3*, 207−211.
(23) Washabaugh, M.; Jencks, W. P. *J. Am. Chem. Soc.* **1989**, *111*, 674−683. Washabaugh, M.; Jencks, W. P. *J. Am. Chem. Soc.* **1989**, *111*, 683−692. Washabaugh, M.; Jencks, W. P. *Biochemistry* **1988**, *27*, 5044−5053.
(24) Kluger, R.; Chin, J.; Smyth, T. J. *J. Am. Chem. Soc.* **1981**, *103*, 884−888.
(25) Knowles, J. R; Albery, W. J. *Biochemistry* **1976**, *15*, 5631−5640.